Journal of Engineering Mathematics **46:** 55–68, 2003.

Propagation of strong converging shock waves in a gas of variable density

G. MADHUMITA and V.D. SHARMA*
Department of Mathematics, Indian Institute of Technology, Powai, Mumbai-400076, India

Received 5 February 2001; accepted in revised form 20 November 2002

Abstract. The problem of a strong converging spherical (or cylindrical) shock collapsing at the centre (or axis) of symmetry is extended to take into account the inhomogeneity of a gaseous medium, the density of which is decreasing towards the centre (or axis) according to a power law. The perturbative approach used in this paper provides a global solution to the implosion problem yielding accurately the results of Guderley's similarity solution, which is valid only in the vicinity of the center/axis of implosion. The analysis yields refined values of the leading similarity parameter along with higher-order terms in Guderley's asymptotic solution near the center/axis of convergence. Computations of the flow field and shock trajectory in the region extending from the piston to the center/axis of collapse have been performed for different values of the adiabatic coefficient and the ambient density exponent.

Key words: asymptotics, implosion, perturbation, self-similar solution, shock wave

1. Introduction

Converging shock waves have been a field of continuing research interest over the years as possible methods for generating high-pressure, high-temperature plasmas at the centre of convergence, as well as to understand the basic fluid dynamics involved in the process. The collapse of an imploding shock wave, which is a remarkable example of a self-similar solution of the second kind, was first analysed by Guderley [1]. Among the extensive work that followed, we mention the contributions by Lazarus and Richtmeyer [2], Van Dyke and Guttmann [3], Hafner [4] and Sakurai [5, 6] who presented high-accuracy results and alternative approaches for the investigation of the implosion problem under consideration.

The present paper demonstrates a successful application of the perturbation-series technique proposed by Van Dyke and Guttmann [3] which provides a global solution to the implosion problem in contrast to Guderley's asymptotic solution that holds only in the vicinity of the center/axis of implosion. We consider a converging shock wave in a non-uniform medium of decreasing density contained in a planar, cylindrical or spherical piston which starts contracting with a velocity greater than the acoustic speed of the medium generating a strong shock inside. Here we study the situation in which a strong converging shock wave propagates through a non-uniform medium of decreasing density and eventually reaches the center/axis where the density vanishes [5]. Such a problem is of great interest in astrophysics as it is highly relevant to the problem of the origin of cosmic rays (see [4–7]). It is well known that near the surface of a star, the density decreases to zero approximately according to a power law $\rho = \rho_c X^\delta$, where X is the distance measured from the surface (see [4], [7],

*Address for correspondence: vsharma@math.iitb.ac.in

[8, Chapter 15]); this density distribution is a result of the combined action of gravity and thermal pressure. In terrestrial problems, such situations may arise for shock waves moving in plasmas sustained by magnetic pressure [7]. The phenomenon is also related in many ways to the shallow-water theory of bores moving up a sloping beach (see [9]).

Our paper is concernd with the investigation of the non-self-similar problem of a strong converging shock wave propagating through a medium with variable density whose distribution is subject to a power law. In addition to the power law behaviour, it is also possible for the gaseous medium to have an exponential density distribution, but in the majority of problems of practical interest, the initial spatial distribution of density is governed by a power-law behaviour ([7, Chapter 12 Section 11], [9, Chapter 5]). We compute the flow field at the rear of the shock wave as it approaches the center/axis of convergence. Computations have been performed for various values of the adiabatic coefficient and the ambient density exponent, and the results are compared with those obtained by using alternative methods.

2. Solution expanded in powers of time

We consider a plane, cylindrical or spherical piston of initial radius R_0 that bounds an ideal gas, the density of which varies initially according to a power law. Let the initial (undisturbed) condition be given by

$$p = p_0, \quad \rho = \rho_c (r/R_0)^{\delta}, \quad v = 0;$$

where r, p, ρ, v are the distance of the particle from the center/axis of symmetry, the pressure, density and the outward radial velocity, respectively, and ρ_c, p_0 and δ are appropriate positive constants.

At time $t = 0$, the piston starts contracting with a constant velocity V, where V is larger than the acoustic speed of the medium; this generates a strong shock wave of planar, cylindrical or spherical geometry whose position has to be determined. The equations of one-dimensional adiabatic motion of an ideal gas have the form:

$$\frac{\partial \rho}{\partial t} + \frac{\partial (\rho v)}{\partial r} + \frac{(j \rho v)}{r} = 0, \tag{1}$$

$$\frac{\partial v}{\partial t} + v \frac{\partial v}{\partial r} + \left(\frac{1}{\rho}\right) \frac{\partial p}{\partial r} = 0, \tag{2}$$

$$\left(\frac{\partial}{\partial t} + v \frac{\partial}{\partial r}\right) \frac{p}{\rho^{\gamma}} = 0, \tag{3}$$

where t is the time, γ is the adiabatic coefficient; j takes values 0, 1 or 2 according to whether the piston is plane, cylindrical or spherical, respectively. In the limit of infinite shock Mach number the boundary conditions immediately behind the shock wave, $r = R(t)$, are given by the Rankine–Hugoniot relations:

$$v = \frac{2}{\gamma + 1} \dot{R}, \qquad \rho = \frac{\gamma + 1}{\gamma - 1} \rho_0, \qquad p = \frac{2}{\gamma + 1} \rho_0 (\dot{R})^2. \tag{4}$$

Here v is the gas velocity relative to the fixed coordinates in which the gas is at rest in a container with radius R_0 and ρ_0 is the undisturbed density of the fluid. The condition of no flow through the piston yields $v = -V$ at $r = R_0 - Vt$. For convenience, we measure the distance inward; let $x = R_0 - r$ and let $u = -v$ be the corresponding velocity directed inward. We introduce the variable

$$y = \frac{2}{\gamma - 1}\left(\frac{x}{Vt} - 1\right), \tag{5}$$

that varies from zero at the piston to unity at the basic position of the shock wave and non-dimensionalize the variables by referring lengths to R_0, speed to V, density to ρ_c, pressure to $\rho_c V^2$ and time to R_0/V. Let the shock front be at a distance X, measured inward from the initial piston location, *i.e.*, $X = R_0 - R$. Thus, the boundary conditions at the shock and piston are, respectively:

$$u = \frac{2}{\gamma + 1}\dot{X}, \quad \rho = \frac{\gamma + 1}{\gamma - 1}(1 - X)^{\delta}, \quad p = \frac{2}{\gamma + 1}(1 - X)^{\delta}\dot{X}^2 \tag{6}$$

at

$$y = \frac{2}{(\gamma - 1)}\left(\frac{X(t)}{t} - 1\right),$$

and

$$u = 1 \quad \text{at} \quad y = 0. \tag{7}$$

Assuming the solution to be analytic in time, we expand the unknown position of the shock wave in a Taylor series in the form:

$$X(t) = \sum_{n=1}^{\infty} X_n t^n, \tag{8}$$

and likewise expand the flow variables in the form:

$$u = \sum_{n=1}^{\infty} U_n(y) t^{n-1}, \quad \rho = \sum_{n=1}^{\infty} R_n(y) t^{n-1}, \quad p = \sum_{n=1}^{\infty} P_n(y) t^{n-1}. \tag{9}$$

Transforming the basic Equations (1)–(3) in the y, t coordinate system and then using the boundary conditions (6) and (7) and the expansions (8) and (9), we find, on equating the coefficients of like powers of t, that the coefficients U_1, R_1 and P_1 for the first approximation remain uninfluenced by the density variations, *i.e.*,

$$U_1 = 1, \quad R_1 = \frac{\gamma + 1}{\gamma - 1}, \quad P_1 = \frac{\gamma + 1}{2}, \quad X_1 = \frac{\gamma + 1}{2}, \tag{10}$$

whilst the coefficients U_2, R_2 and P_2 for the second approximation which exhibit δ-dependence satisfy the following first-order linear ordinary differential equations and boundary conditions,

$$\frac{\gamma + 1}{\gamma - 1}U_2' - \frac{(\gamma - 1)yR_2'}{2} + \frac{(\gamma - 1)R_2}{2} = \frac{j(\gamma + 1)}{2}, \tag{11}$$

$$\frac{(\gamma + 1)yU_2'}{2} - \frac{(\gamma + 1)U_2}{2} - P_2' = 0, \tag{12}$$

$$y\left[\frac{\gamma + 1}{\gamma - 1}P_2' - \frac{\gamma(\gamma + 1)}{2}R_2'\right] - \frac{\gamma + 1}{\gamma - 1}P_2 + \frac{\gamma(\gamma + 1)}{2}R_2 = 0, \tag{13}$$

$$U_2(1) = \frac{4X_2}{\gamma + 1}, \quad P_2(1) = 4X_2 - \frac{\delta(\gamma + 1)^2}{4}, \quad R_2(1) = -\frac{\delta(\gamma + 1)^2}{2(\gamma - 1)}. \tag{14}$$

Here a prime denotes derivative with respect to y. Eliminating P_2 from (12) and (13) we have an equation in U_2 and R_2. This together with (11) and the boundary conditions (7) and (14) can be solved to yield U_2 and hence P_2 and R_2. Thus, the second-order approximation is as follows:

$$U_2 = \frac{y}{2}\frac{(\gamma-1)}{(2\gamma-1)}\left(j\gamma + \delta\frac{\gamma+1}{2}\right), \tag{15}$$

$$R_2 = \frac{\gamma+1}{2\gamma-1}\left[\left(j - \frac{\delta}{2}\frac{(\gamma+1)}{(\gamma-1)}\right) - y(j+\delta(\gamma+1)\right)\right], \tag{16}$$

$$P_2 = \frac{\gamma(\gamma+1)}{2(2\gamma-1)}\left[j(\gamma-1) - \frac{\delta(\gamma+1)}{2}\right], \tag{17}$$

$$X_2 = \frac{(\gamma+1)(\gamma-1)}{8(2\gamma-1)}\left[j\gamma + \delta\frac{(\gamma+1)}{2}\right]. \tag{18}$$

Equations (15)–(18) suggest that the coefficients U_n, R_n and P_n are polynomials in y of the form:

$$U_n(y) = \sum_{k=2}^{n} U_{nk}y^{k-1}, \quad R_n(y) = \sum_{k=1}^{n} R_{nk}y^{k-1}, \quad P_n(y) = \sum_{k=1}^{n} P_{nk}y^{k-1}. \tag{19}$$

Substituting these in the transformed form of the basic differential Equations (1)–(3) in the (y,t) plane and the shock conditions (6), we have for the nth approximation a system of $3n$ linear algebraic equations in the coefficients U_{nk}, R_{nk}, P_{nk} and X_n. For the third-order approximation, we have the following system of ordinary differential equations and the associated boundary conditions,

$$\frac{\gamma+1}{\gamma-1}U_3{}' - \frac{(\gamma-1)y}{2}R_3' + (\gamma-1)R_3 + Ay + B = 0,$$

$$P_3' - \frac{(\gamma+1)y}{2}U_3' + (\gamma+1)U_3 + Cy = 0,$$

$$\frac{(\gamma+1)y}{2}P_3' - (\gamma+1)P_3 - \frac{\gamma(\gamma-1)(\gamma+1)}{4}yR_3' + \frac{\gamma(\gamma-1)(\gamma+1)}{2}R_3 - A_1y - B_1 = 0,$$

$$U_3(1) = \frac{6X_3}{\gamma+1} - \frac{\gamma^2-1}{8(2\gamma-1)^2}(j\gamma + \delta\frac{\gamma+1}{2})^2,$$

$$R_3(1) = \frac{\delta(\gamma+1)^2}{8}\left[\frac{(\gamma+1)(\delta-1)}{\gamma-1} - \frac{j\gamma+\delta(\gamma+1)/2}{2\gamma-1}\right] + \frac{(\gamma+1)^2}{4(2\gamma-1)^2}\left[j\gamma + \delta\frac{(\gamma+1)}{2}\right](j+\delta(\gamma+1)),$$

$$P_3(1) = -\frac{5\delta(\gamma+1)^2(\gamma-1)}{16(2\gamma-1)}\left[j\gamma + \delta\frac{(\gamma+1)}{2}\right] + \frac{\delta(\delta-1)(\gamma+1)^3}{8} + \frac{(\gamma+1)(\gamma-1)^2}{8(2\gamma-1)^2}\left(j\gamma + \delta\frac{\gamma+1}{2}\right)^2 + 6X_3,$$

where

$$A=-\frac{(\gamma+1)(\gamma-1)}{4(2\gamma-1)^2}\left[j^2(2\gamma^2-\gamma+2)+j\left(\frac{\delta(\gamma+1)(2\gamma+7)}{2}+(2\gamma-1)^2\right)+2\delta^2(\gamma+1)^2\right],$$

$$B=\frac{(\gamma+1)(\gamma-1)}{2(2\gamma-1)^2}\left[-j^2(\gamma-1)+j\left(\delta(\gamma+1)-\frac{(2\gamma-1)^2}{\gamma-1}\right)-\frac{\delta^2}{4}\frac{(\gamma+1)^2}{(\gamma-1)}\right],$$

$$C=\frac{(\gamma-1)(\gamma+1)}{4(2\gamma-1)^2}\left(j\gamma+\delta\frac{\gamma+1}{2}\right)^2,$$

$$A_1=\frac{\gamma(\gamma-1)(\gamma+1)^2}{4(2\gamma-1)^2}(j+\delta(\gamma+1))^2,$$

$$B_1=-\frac{\gamma(\gamma-1)^3(\gamma+1)^2}{4(2\gamma-1)^2}\left(j-\frac{\delta}{2}\frac{(\gamma+1)}{(\gamma-1)}\right)^2.$$

The solution of the above system yields the position of the shock wave up to the third-order approximation as

$$\begin{aligned}X(t)=\ &\frac{(\gamma+1)t}{2}+\frac{(\gamma+1)(\gamma-1)}{8(2\gamma-1)}\left[j\gamma+\delta\frac{(\gamma+1)}{2}\right]t^2\\&+\frac{(\gamma-1)(\gamma+1)}{48(7\gamma-5)}[j^2\frac{\gamma(13\gamma^3-21\gamma^2+13\gamma-1)}{(2\gamma-1)^2}\\&+j(\gamma+1)(3\gamma+1)+j\frac{\delta(\gamma+1)(28\gamma^3-43\gamma^2+26\gamma-1)}{2(2\gamma-1)^2}\\&+\frac{\delta^2(\gamma+1)^2(47\gamma^2-54\gamma+19)}{4(2\gamma-1)^2}-4\delta(\delta-1)(\gamma+1)^2]t^3+O(t^4).\end{aligned}$$

In the absence of density stratification ($\delta=0$), the above result reduces to the one obtained by Van Dyke and Guttmann [3] for a uniform-density fluid. As the hand calculations become very tedious after the third approximation, we compute the succeeding terms of the series solution for the shock position with the help of a computer program.

3. Computer-extended series

We have written a program using the software package Mathematica. The program has two parts. In the first part, we generated a system of algebraic equations using (9) and (19). In the second part, these equations are solved to give the values of U_{nk}, R_{nk} and P_{nk} and X_n. We have done the entire calculation using rational arithmetic for plane, cylindrical and spherical geometries with adiabatic coefficient $\gamma=7/5$ and 5/3 and with density exponent $\delta=1$ and 2. Table 1 lists the first forty-one coefficients in the series expansion for the shock location for $\gamma=5/3$ and $\delta=2$ for plane ($j=0$), cylindrical ($j=1$) and spherical ($j=2$) symmetry. Although we have shown the coefficients rounded to 12 significant digits, we have carried out all the subsequent calculations using 32 significant digits. This reduces the effect of round-off errors and truncation errors to a great extent.

Table 1. Coefficients X_n in the expansion (8) for the radius of the shock wave position when $\gamma = 5/3$ and $\delta = 2$.

n	Planar	Cylindrical	Spherical
1	1·333333333333	1·333333333333	1·333333333333
2	0·253968253968	0·412698412698	0·571428571429
3	0·274124464601	0·535147392290	0·872763920383
4	0·299463700824	0·676712777998	1·259449890087
5	0·354952943572	0·950192741054	2·054352043110
6	0·460141586279	1·474158698972	3·711153927337
7	0·636322437666	2·413162851141	6·989421070721
8	0·916953105025	4·082594041918	13·56417933179
9	1·359823836778	7·095656513587	27·06229357367
10	2·062810898079	12·60752886369	55·12392665063
11	3·188121061213	22·79258651799	114·0679337561
12	5·003399686395	41·78636222250	239·1994508056
13	7·952444403837	77·51410005438	507·2856774155
14	12·77551498173	145·2368139327	1086·060369030
15	20·71294720773	274·4736210016	2344·085751087
16	33·85060541023	522·5817368999	5095·195640129
17	55·70844949638	1001·471720138	11143·92982915
18	92·24640843343	1930·301295556	24506·95733389
19	153·5873046382	3739·705420168	54156·83804849
20	256·9741833924	7278·514448997	120201·8071397
21	431·8571286486	14224·71060024	267839·5857984
22	728·6605963921	27904·21533474	598940·1468991
23	1233·922695953	54925·63786969	$1{\cdot}343686439900 \times 10^{6}$
24	2096·483451574	108450·5052810	$3{\cdot}023410959663 \times 10^{6}$
25	3572·861090717	214747·1354689	$6{\cdot}821423033776 \times 10^{6}$
26	6105·998998068	426347·7787154	$1{\cdot}542900151460 \times 10^{7}$
27	10462·12825770	848504·6874548	$3{\cdot}497863948749 \times 10^{7}$
28	17968·97065493	$1{\cdot}692468245463 \times 10^{6}$	$7{\cdot}946878824199 \times 10^{7}$
29	30930·87426125	$3{\cdot}382934178896 \times 10^{6}$	$1{\cdot}809060199772 \times 10^{8}$
30	53353·22188845	$6{\cdot}775028511990 \times 10^{6}$	$4{\cdot}125847110127 \times 10^{8}$
31	92208·04330716	$1{\cdot}359306134277 \times 10^{7}$	$9{\cdot}425919459996 \times 10^{8}$
32	159647·7014035	$2{\cdot}731878605689 \times 10^{7}$	$2{\cdot}156933293360 \times 10^{9}$
33	276881·0908831	$5{\cdot}499175864376 \times 10^{7}$	$4{\cdot}943203513062 \times 10^{9}$
34	480967·9980374	$1{\cdot}108623762300 \times 10^{8}$	$1{\cdot}134486642876 \times 10^{10}$
35	836740·3824990	$2{\cdot}238118390354 \times 10^{8}$	$2{\cdot}607193190253 \times 10^{10}$
36	$1{\cdot}457739161644 \times 10^{6}$	$4{\cdot}524383502613 \times 10^{8}$	$5{\cdot}999248662023 \times 10^{10}$
37	$2{\cdot}543017916727 \times 10^{6}$	$9{\cdot}157592571039 \times 10^{8}$	$1{\cdot}382101615324 \times 10^{11}$
38	$4{\cdot}441894526034 \times 10^{6}$	$1{\cdot}855749817738 \times 10^{9}$	$3{\cdot}187679369510 \times 10^{11}$
39	$7{\cdot}767968684102 \times 10^{6}$	$3{\cdot}764841465896 \times 10^{9}$	$7{\cdot}359954192203 \times 10^{11}$
40	$1{\cdot}360004931043 \times 10^{7}$	$7{\cdot}646067796961 \times 10^{9}$	$1{\cdot}701052266506 \times 10^{12}$
41	$2{\cdot}383651026655 \times 10^{7}$	$1{\cdot}554428223524 \times 10^{10}$	$3{\cdot}935322135061 \times 10^{12}$

The computed results in the neighbourhood of collapse are in agreement with the exact numerical results (see Table 7). In what follows next, similar tables for other values of j, γ and δ have not been given for brevity.

4. Refinement of the radius of convergence

The coefficients of first 41 terms in the expansion (8) for the radius of the shock wave indicate that the radius of convergence of the series is less than unity. At the instant $t = 1$ the piston itself would reach the axis and the power-series solution breaks down. We shall investigate whether this singularity corresponds to Guderley's singularity. Assuming that the shock wave admits Guderley's similarity solution near the point of its collapse, we find that the shock position is given by

$$R(t) = 1 - X(t) = 1 - \sum X_n t^n \sim A_1 \left(1 - \frac{t}{t_c}\right)^{\alpha_1} \quad \text{as} \quad t \to t_c. \tag{20}$$

Thus,

$$\frac{X_n}{X_{n-1}} \sim \frac{1}{t_c}\left(1 - \frac{1+\alpha_1}{n}\right) \quad \text{as} \quad n \to \infty,$$

where t_c represents the time taken by the shock to collapse. We assume that, when n is large, the ratio X_n/X_{n-1} approximates the value of $1/t_c$. Under this assumption we construct a sequence X_n/X_{n-1} ($n = 32, 33, \ldots, 41$) and thereafter refine this estimate of $1/t_c$ by forming a Neville Table in the usual manner. Given a sequence e_n^0, we can construct a triangular array of elements e_n^r, where n labels the rows and $r = 0, 1, 2, 3, \ldots, n$ labels the columns. The elements of the rth column are generated from the $(r-1)$th column by using the form [10]:

$$e_n^r = \frac{n e_n^{r-1} - (n-r) e_{n-1}^{r-1}}{r}. \tag{21}$$

Here $r = 1$ corresponds to linear intercepts, $r = 2$ to quadratic intercepts, $r = 3$ to the cubic intercepts, and so on. The Neville table so formed provides a refined estimate for e_n^0. In order to construct a Neville table for $1/t_c$, we compute the sequence X_n/X_{n-1} ($n = 32, 33, \ldots, 41$) and take this as the initial sequence e_n^0; this comprises the first column of Table 2. Then using (21), we compute the sequence e_n^1 ($n = 33, 34, \ldots, 41$) and this gives the second column of Table 2. Likewise, all successive columns of the Neville table are formed, which show that the sequences $e_n^0, e_n^1, e_n^2, \ldots$ approach a limiting value $1/t_c$.

From Tables 2 and 3 the values of $1/t_c$ and α_1 for a cylindrical piston with $\gamma = 5/3$ and $\delta = 2$ are 2·115512 and 0·5994, respectively. Though the estimate for $1/t_c$ is reasonably good, we can refine the results as follows. As observed earlier, the radius of convergence of the series solution is less than unity. At the instant, $X(t) = 1$, the series solution breaks down and the shock wave collapses. Hence the real root of the equation $X(t) = \sum_1^N X_n t^n = 1$ gives a rough estimate of t_c, which has been evaluated with the help of Mathematica for $N = 32, 33, 34, \ldots, 41$. Constructing a Neville table with these roots as the initial sequence e_n^0, we find that the successive sequences yield a more accurate value of t_c as compared to the one obtained from Table 2. The value of t_c obtained from Table 4 for $j = 1$, $\gamma = 5/3$, and $\delta = 2$ is 0·47269876; values of t_c for different values of γ, j and δ are given in Table 5.

Table 2. The Neville table for estimating the reciprocal of the radius of convergence $1/t_c$ for $j = 1,\ \gamma = 5/3$ and $\delta = 2$.

n	e_n^0	Linear	Quadratic	Cubic	Quartic
37	2·02405313	2·11552852	2·11550581	2·11551263	2·11551451
38	2·02646034	2·11552736	2·11550633	2·11551238	2·11551027
39	2·02874408	2·11552630	2·11550678	2·11551228	2·11551136
40	2·03091362	2·11552535	2·11550720	2·11551232	2·11551272
41	2·03297730	2·11552448	2·11550757	2·11551233	2·11551238

Table 3. The Neville table for the similariry exponent α_1 for $j = 1,\ \gamma = 5/3$ and $\delta = 2$.

n	e_n^0	Linear	Quadratic	Cubic	Quartic
37	0·599602528	0·599321334	0·599423795	0·599413701	0·599374529
38	0·599595269	0·599326699	0·599423256	0·599416969	0·599444747
39	0·599588509	0·599331630	0·599422865	0·599418174	0·599428715
40	0·599582201	0·599336169	0·599422411	0·599416808	0·599404520
41	0·599576302	0·599340354	0·599421949	0·599416094	0·599409488

Table 4. The Neville table for estimating the radius of convergence t_c for $j = 1,\ \gamma = 5/3$ and $\delta = 2$.

n	Linear	Quadratic	Cubic	Quartic	Quintic
37	0·472675036	0·472699141	0·472698783	0·472698760	0·472698749
38	0·472676303	0·472699112	0·472698780	0·472698758	0·472698749
39	0·472677471	0·472699087	0·472698778	0·472698757	0·472698749
40	0·472678551	0·472699063	0·472698776	0·472698756	0·472698748
41	0·472679550	0·472699042	0·472698774	0·472698755	0·472698748

Table 5. Values of t_c, the time taken by the shock to collapse, for $\gamma = 7/5,\ 5/3$ and $\delta = 1,\ 2$.

γ	δ	t_c(Planar)	t_c(Cylindrical)	t_c(Spherical)
7/5	1	0·8	0·62560203	0·5522584
7/5	2	0·6311728	0·5562757	0·49695567
5/3	1	0·63322227	0·536922155	0·46570332
5/3	2	0·54694133	0·47269876	0·416159476

5. Structure of the local singular solution

Guderley [1] conjectured that in the neighbourhood of collapse, the shock location can be described by an expansion:

$$R(t) = 1 - X(t) \sim \sum_{i=1} A_i \left(1 - \frac{t}{t_c}\right)^{\alpha_i}. \tag{22}$$

He computed only the first exponent α_1; the remaining exponents and amplitudes were unknown. Van Dyke and Guttmann [3] successfully computed all the real exponents and the corresponding amplitudes for an ideal gas using the method of Baker and Hunter [11]; the latter have devised a technique for detecting confluent singularities when an accurate estimate of the location of the dominant singularity is available. This involves the creation of an auxiliary function from the given function. In (22), we substitute the value of t_c obtained in the previous section and introduce an auxiliary variable τ given by $t = t_c(1 - \exp(-\tau))$; thereafter, we multiply the nth term by $n!$ and sum over n to obtain the series for an auxiliary function

$$\mathcal{R}(\tau) = \sum_{i=1} A_i/(1 + \alpha_i \tau), \tag{23}$$

which has poles at $-1/\alpha_i$ and corresponding residues A_i/α_i, and is of the form of an $[(N - 1)/N]$ Pade approximant [12, Chapter 1]. This is, indeed, a rational function approximant to a Taylor series expansion given as the ratio of two polynomials, the coefficients of which are constructed from the series solution. As we have a series with approximately 40 terms, N can be varied up to 20 at the most. Varying N from 3 to 20, we get the successive $[(N-1)/N]$ approximants to the auxiliary function, $\mathcal{R}(\tau)$. Splitting these approximants into partial fractions, we get the values of α_i and A_i which constitute a list of admissible similarity exponents and the corresponding amplitudes recovered in the neighbourhood of collapse. This entire work of transforming the function $R(t)$ to an auxiliary function $\mathcal{R}(\tau)$, forming the Pade approximants, and then splitting the same into partial fractions has been carried out using Mathematica. The exponents and amplitudes obtained from the poles and residues of these fractions are listed in Table 6.

6. Concluding Remarks

A problem involvong a converging shock wave has been formulated with a gas of varying density obeying a power law. The entire flow field extending from the piston to the center/axis of collapse, where Guderley's local analysis cannot provide the solution, is analysed using the perturbation approach proposed by Van Dyke and Guttmann [3]. The global solution confirms Guderley's local self-similar solution near the center/axis and yields refined values of the similarity parameter along with higher order terms in Guderley's expansion; the values of the first three similarity exponents and amplitudes in Guderley's local expansion are extracted from the coefficients in our perturbative series, and are listed in Table 6. The values of the leading exponent α_1 for different values of j, γ and δ are given in Table 7; these compare well with the numerical results obtained in Refs. [4], [5] and [13]. The fact that α_1 is always less than unity shows that the shock is continuously accelerated; in fact the shock speed becomes unbounded as $t \to t_c$, but less rapidly than $(t - t_c)^{-1}$. We notice that an increase in any of the parameters j, γ or δ causes the leading similarity exponent α_1 to decrease and consequently brings about an increase in the shock acceleration as it approaches the center/axis.

Table 6. Similarity exponents and corresponding amplitudes for different j, γ and δ.

j	γ	δ	Exponents	Amplitudes
0	7/5	1	$\alpha_1 = 0{\cdot}831852044124997$	$A_1 = \ 0{\cdot}974097989030041$
			$\alpha_2 = 2{\cdot}204296521077008$	$A_2 = \ 0{\cdot}02951627083958669$
			$\alpha_3 = 3{\cdot}179268335989584$	$A_3 = -0{\cdot}00346439212730139$
0	7/5	2	$\alpha_1 = 0{\cdot}7176988659369873$	$A_1 = \ 0{\cdot}97452123056781$
			$\alpha_2 = 2{\cdot}388425655181384$	$A_2 = \ 0{\cdot}0277749479851510$
			$\alpha_3 = 3{\cdot}582478345092601$	$A_3 = -0{\cdot}000995715219429995$
0	5/3	1	$\alpha_1 = 0{\cdot}817428265131909$	$A_1 = \ 0{\cdot}977893654931644$
			$\alpha_2 = 2{\cdot}128657585030641$	$A_2 = \ 0{\cdot}0241564736779048$
			$\alpha_3 = 3{\cdot}158336713747037$	$A_3 = -0{\cdot}002024200002912269$
0	5/3	2	$\alpha_1 = 0{\cdot}6965814555233822$	$A_1 = \ 0{\cdot}978099342412351$
			$\alpha_2 = 2{\cdot}261889612239047$	$A_2 = \ 0{\cdot}02330367149114996$
			$\alpha_3 = 3{\cdot}22910421177461$	$A_3 = \ 0{\cdot}004632978257337105$
1	7/5	1	$\alpha_1 = 0{\cdot}7149227872587102$	$A_1 = \ 0{\cdot}976215584035954$
			$\alpha_2 = 2{\cdot}205325727678336$	$A_2 = \ 0{\cdot}02301857273630043$
			$\alpha_3 = 3{\cdot}770302627342177$	$A_3 = \ 0{\cdot}00834259484380019$
1	7/5	2	$\alpha_1 = 0{\cdot}6283413666826567$	$A_1 = \ 0{\cdot}977445447015596$
			$\alpha_2 = 2{\cdot}366114588765389$	$A_2 = \ 0{\cdot}0222480063136541$
1	5/3	1	$\alpha_1 = 0{\cdot}6883735502859699$	$A_1 = \ 0{\cdot}980579710047778$
			$\alpha_2 = 2{\cdot}049627009839459$	$A_2 = \ 0{\cdot}01824624027483898$
			$\alpha_3 = 3{\cdot}319517895915208$	$A_3 = \ 0{\cdot}003515148017073944$
1	5/3	2	$\alpha_1 = 0{\cdot}5994460186251939$	$A_1 = \ 0{\cdot}980754849682343$
			$\alpha_2 = 2{\cdot}167020972574668$	$A_2 = \ 0{\cdot}01861425008290034$
2	7/5	1	$\alpha_1 = 0{\cdot}6266778045095402$	$A_1 = \ 0{\cdot}978749222955747$
			$\alpha_2 = 2{\cdot}191031361851746$	$A_2 = \ 0{\cdot}0170757777249875$
			$\alpha_3 = 2{\cdot}334752854004494$	$A_3 = \ 0{\cdot}001898006877797207$
2	7/5	2	$\alpha_1 = 0{\cdot}5588081764878352$	$A_1 = \ 0{\cdot}97995544166925$
			$\alpha_2 = 2{\cdot}344712136174166$	$A_2 = \ 0{\cdot}01839683827762583$
2	5/3	1	$\alpha_1 = 0{\cdot}5946705012670877$	$A_1 = \ 0{\cdot}983187083610092$
			$\alpha_2 = 1{\cdot}988678822962598$	$A_2 = \ 0{\cdot}0143883512470273$
			$\alpha_3 = 3{\cdot}351885536569706$	$A_3 = \ 0{\cdot}0290805285641347$
2	5/3	2	$\alpha_1 = 0{\cdot}5263859655114837$	$A_1 = \ 0{\cdot}983095597303395$
			$\alpha_2 = 2{\cdot}093892914192529$	$A_2 = \ 0{\cdot}01530040019401947$

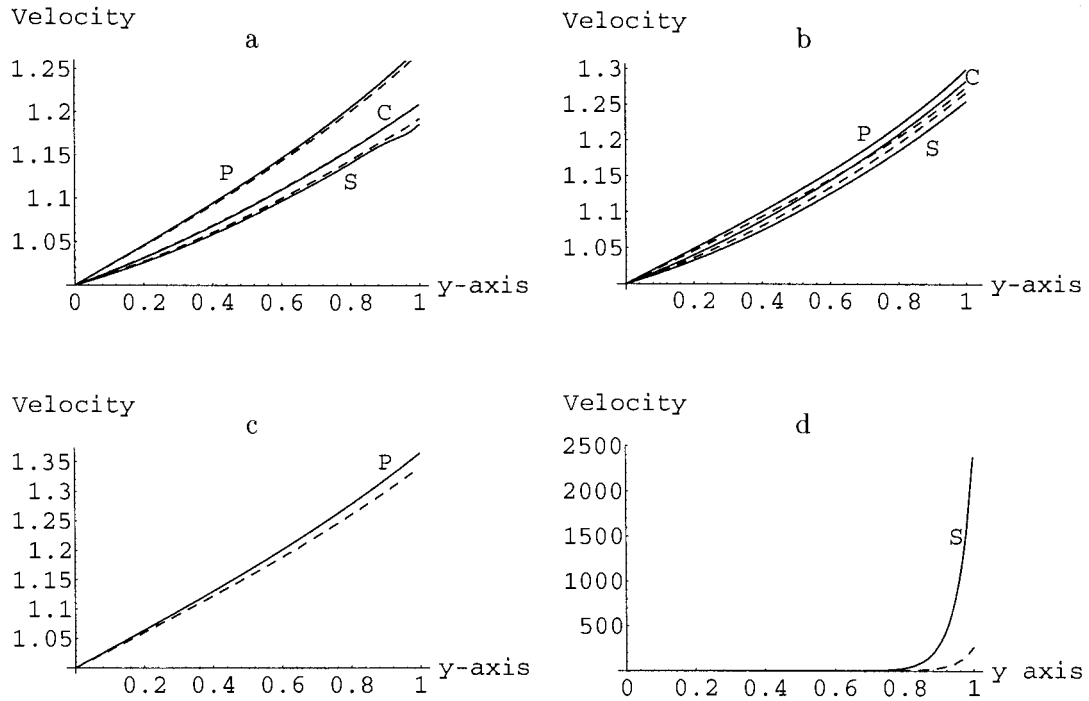

Figure 1. (a-d): Velocity profiles for planar (P), cylindrical (C) and spherical (S) geometries. The solid and dashed lines indicate the flow profiles at the time of collapse $t = t_c$, and just before collapse $t = t_{bc}$, respectively. (a) determines the flow profiles for $\gamma = 7/5, \delta = 1$; for the planar flow P: $t_c = 0{\cdot}8, t_{bc} = 0{\cdot}79$; for the cylindrical flow C: $t_c = 0{\cdot}6256, t_{bc} = 0{\cdot}61$; for the spherical flow S: $t_c = 0{\cdot}55225, t_{bc} = 0{\cdot}54$; (b) represents the velocity profiles for $\gamma = 5/3, \delta = 2$; for P: $t_c = 0{\cdot}6332, t_{bc} = 0{\cdot}61$; for C: $t_c = 0{\cdot}5369, t_{bc} = 0{\cdot}51$; for S: $t_c = 0{\cdot}4657, t_{bc} = 0{\cdot}44$; (c-d) represent the velocity profiles for $\gamma = 5/3, \delta = 2$; for P: $t_c = 0{\cdot}5469, t_{bc} = 0{\cdot}52$; for S: $t_c = 0{\cdot}4161, t_{bc} = 0{\cdot}39$.

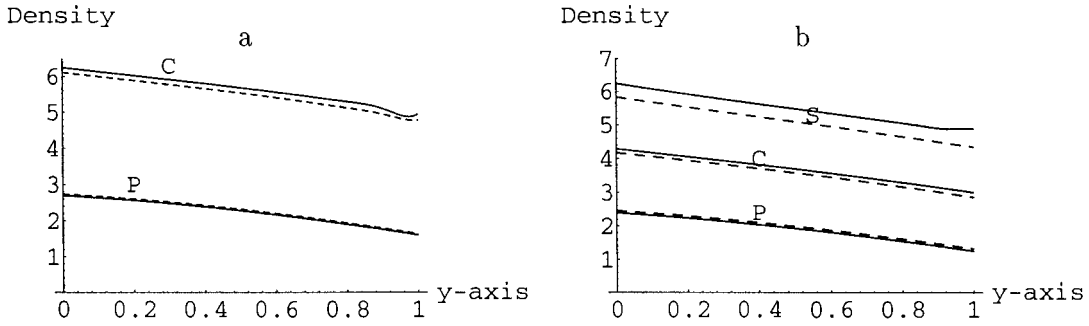

Figure 2. (a,b): Density profiles for the three symmetries. The solid and dashed lines indicate the density at t_c and t_{bc} respectively. (a) represents the density profiles for $\gamma = 7/5, \delta = 1$; for P: $t_c = 0{\cdot}8, t_{bc} = 0{\cdot}79$; for C: $t_c = 0{\cdot}6256, t_{bc} = 0{\cdot}61$; (b) gives the density profiles for $\gamma = 5/3, \delta = 1$; for P: $t_c = 0{\cdot}6332, t_{bc} = 0{\cdot}61$; for C: $t_c = 0{\cdot}5369, t_{bc} = 0{\cdot}51$; for S: $t_c = 0{\cdot}4657, t_{bc} = 0{\cdot}44$.

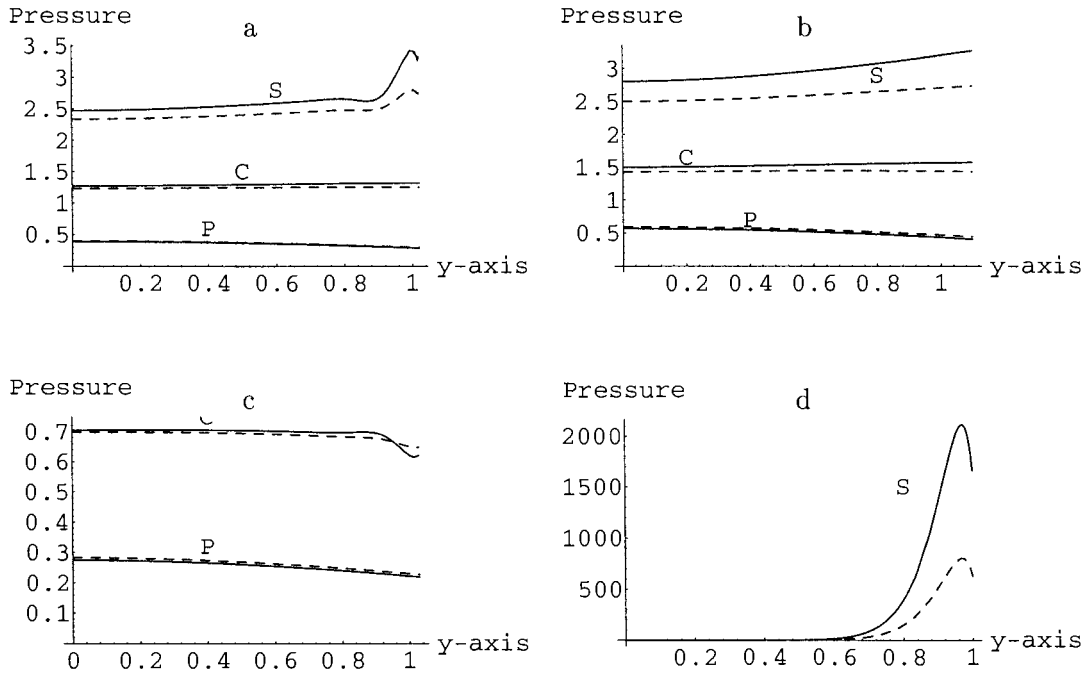

Figure 3. (a-d): Pressure profiles for the three symmetries. (a) represents the flow profiles for $\gamma = 7/5, \delta = 1$; for P:$t_c = 0{\cdot}8, t_{bc} = 0{\cdot}79$; for C: $t_c = 0{\cdot}6256, t_{bc} = 0{\cdot}61$; for S: $t_c = 0{\cdot}55225, t_{bc} = 0{\cdot}54$; (b) denotes the flow profiles for $\gamma = 5/3, \delta = 1$; for P: $t_c = 0{\cdot}6332, t_{bc} = 0{\cdot}61$; for C: $t_c = 0{\cdot}5369, t_{bc} = 0{\cdot}51$; for S: $t_c = 0{\cdot}4657, t_{bc} = 0{\cdot}44$; (c-d) represent the pressure profiles for $\gamma = 7/5, \delta = 2$; for P: $t_c = 0{\cdot}6311, t_{bc} = 0{\cdot}62$; for C: $t_c = 0{\cdot}5562, t_{bc} = 0{\cdot}54$; for S: $t_c = 0{\cdot}4969, t_{bc} = 0{\cdot}48$.

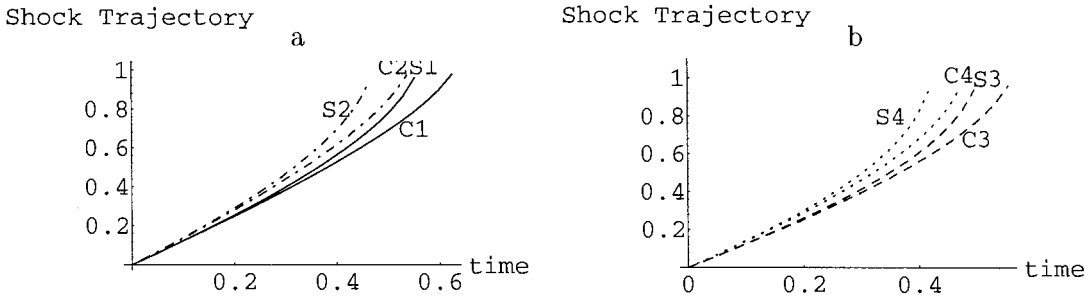

Figure 4. (a): C1 and S1 represent the shock trajectories for cylindrical and spherical flow fields for $\gamma = 7/5, \delta = 1$; C2 and S2 represent the cylindrical and spherical shock paths for $\gamma = 5/3, \delta = 1$. (b): C3 and S3 denote the cylindrical and spherical shock profiles for $\gamma = 7/5, \delta = 2$ while C4 and S4 denote the cylindrical and spherical shock profiles for $\gamma = 5/3, \delta = 2$.

The flow variables are computed to elucidate the effects of varying the adiabatic coefficient, the wavefront curvature and the density stratification. Figures 1(a–d) and 2(a–b) show that the velocity decreases monotonically behind the shock as we move towards the piston, whereas the density exhibits an increasing trend in the region behind the shock; this is on account of geometrical convergence or area contraction of the shock wave which causes velocity to decrease and density to increase. It is found that an increase in γ or δ results in an increase in the particle velocity and a decrease in the density (see Figures 1 and 2). It may be noticed that for spherically symmetric flows the velocity distribution becomes steeper as compared to

Table 7. Comparison of the computed value of the dominant similarity exponent α_1 with those obtained by the other authors.

j	γ	δ	Computed α_1	Sharma and Radha [13]	Hafner [4]	Sakurai [5]
0	7/5	1	0·831852044124997	0·831848815918	0·831851098197583	0·831849867
0	7/5	2	0·7176988659369873	0·717696691895	0·717699788037417	0·717699915
0	5/3	1	0·817428265131909	0·817425122070	0·817427518983985	0·817427555
0	5/3	2	0·6965814555233822	0·696577789307	0·696581002711928	0·696582565
1	7/5	1	0·7149227872587102	0·7147654371895		
1	7/5	2	0·6283413666826567	0·6283397583008	0·628341718080 387	
1	5/3	1	0·6883735502859699	0·6883719325065		
1	5/3	2	0·5994460186251939	0·5994441223144	0·599446006340436	
2	7/5	1	0·6266778045095402	0·626676673889		
2	7/5	2	0·5588081764878352	0·558805505371	0·558808169990111	
2	5/3	1	0·5946705012670877	0·594669113159		
2	5/3	2	0·5263859655114837	0·526383563232	0·526385934682883	

the planar flows when $\delta = 2$. A more pronounced indication of this behaviour can be seen as the front approaches the center/axis (see Figure 1(d)); indeed the amplification mechanism of flow convergence is stronger for the spherical case than for a planar or cylindrical geometry. The results indicate that the gas pressure remains bounded in the region behind the shock; indeed, it is stationary in most of the region except in the vicinity of the front where it attains a maximum. This is due to the fact that the gas which is highly compressed by the shock, cools down in the region behind the shock, and the density ahead of the front decreases at the same rate at which the square of the front velocity increases. It is observed that an increase in γ or δ causes the gas pressure to increase in the region behind the shock (see Figures 3(a–d)); indeed the stationary values of the gas pressure become larger as the front approaches the center/axis. Figures 4(a–b) indicate that in the initial stage, in the neighbourhood of the piston, spherical and cylindrical shock trajectories coincide, indicating that the geometrical convergence effects are small initially at large radii; in fact the shocks gradually accelerate in the intermediate region and then rapidly do so near the centre of symmetry as a result of adiabatic compression of the shocked state due to flow area convergence.

Acknowledgement

This research work was supported by CSIR research grant No. 25(0122)/02/EMR-II.

References

1. G. Guderley, Kugelige and Zylindrische Verdichtungsstosse in der Nake des Kugelmittelpunktes Lzw der Zylinderachse. *Luftfahrtforschung* 19 (1942) 302–312.
2. R.B. Lazarus, and R.D. Richtmeyer, Similarity solutions for converging shocks. *Los Alamos Scientific Lab. Rep.* LA-6823-MS (1977).
3. M. VanDyke and A.J. Guttmann, The converging shock wave from a spherical or cylindrical piston. *J. Fluid Mech.* 120 (1982) 451–462.

4. P. Hafner, Strong convergent shock waves near the centre of convergence: A power series solution. *SIAM J. Appl. Math* 48 (1988) 1244–1261.
5. A. Sakurai, On the problem of a shock wave arriving at the edge of a gas. *Comm. Pure Appl. Math.* 13 (1960) 353–370.
6. A. Sakurai, Propagation of spherical shock waves in stars. *J. Fluid Mech.* 1 (1956) 436–453.
7. Ya.B. Zeldovich and Yu.P. Raizer, *Physics of Shock Waves and High Temperature Hydrodynamic Phenomena* Vol. II. New York: Academic (1967) pp. 465–916.
8. K.P. Stanyukovich, *Unsteady Motion of Continuous Media*. Oxford: Pergamon (1960) 745 pp.
9. J.J. Stoker, *Water Waves*. New York: Interscience Publishers (1957) 567 pp.
10. D.S. Gaunt and A.J. Guttmann, Asymptotic analysis of coefficients. In: C. Domb and M.S.Green (eds.), *Phase Transitions and Critical Phenomena* 3. New York: Academic (1974) 181–243 pp.
11. G.A. Baker and D.L. Hunter, Methods of series analysis II. Generalized and extended methods with applications to the ising model. *Phys. Rev.* B7 (1978) 3377–3392.
12. G.A. Baker Jr., *Essentials of Pade Approximants*. London: Academic (1975) 306 pp.
13. V.D. Sharma and Ch. Radha, Similarity solutions for converging shock in a relaxing gas. *Int. J. Engg. Sciences* 33 (1995) 535–553.